



# Chapter 14

## In Vitro Assessment of Mitochondrial Toxicity to Predict Drug-Induced Liver Injury

Mathieu Porceddu, Nelly Buron, Pierre Rustin, Bernard Fromenty, and Annie Borgne-Sanchez

### Abstract

Mitochondrial liability of drugs and other xenobiotics is a major issue for patients because such toxicity can damage different tissues and organs such as liver, heart, and muscle. Drug-induced mitochondrial toxicity is also a major concern for pharmaceutical industries. Indeed, it is now acknowledged that such mechanism of toxicity can induce severe, and sometimes fatal, liver injury which can lead to the interruption of clinical trials, or drug withdrawal after marketing, such as in the case of troglitazone. Therefore, drug-induced mitochondrial dysfunction is increasingly sought after by pharmaceutical companies by using reliable in vitro assays in order to discard potential mitochondrion-toxic drugs during drug discovery stage. This chapter presents the in vitro methods used to identify potential mitochondrion-toxic drugs. To this end, different types of biological materials are used such as isolated mouse liver mitochondria and the human hepatic HepaRG<sup>®</sup> cell line, which expresses the main enzymes and transcription factors involved in drug metabolism. The in vitro method we discussed allows to investigate several key mitochondrial parameters such as oxygen consumption, transmembrane potential, respiratory chain complex activities, and mtDNA levels. These investigations are able to detect not only direct and acute mitochondrial alterations due to parent drugs but also indirect and chronic mitochondrial liability that can be induced by secondary metabolites. Hence, it could be used to detect potential drug-induced mitochondrial liability and to understand the involved mechanisms.

**Key words** DILI, Drug-induced liver injury, Hepatocytes, Hepatotoxicity, Liver, Mitochondria, Mitochondrial toxicity, Oxidative stress, Respiratory chain, Transmembrane potential

---

## 1 Introduction

Mitochondrial toxicity of drugs and other xenobiotics is a major issue for patients because such toxicity can induce acute or chronic injury involving different organs and tissues such as liver, heart, muscle, kidney and adipose tissues [1–3]. In the worst scenario, these diseases can lead to long-term hospitalization and death of the patients. Ethanol consumed in excess amounts by millions of individuals all over the world is known for a long time to favor the occurrence of different liver diseases by altering mitochondrial

function by different mechanisms [4–6]. Although still scarce, some studies also suggest that exposure to environmental contaminants such as bisphenol A and benzo[a]pyrene results in mitochondrial dysfunction [7, 8].

In addition to the public health issue, drug-induced mitochondrial toxicity is also a major concern for pharmaceutical industries. Indeed, mitochondrial liability has been pinpointed for severe adverse events and deaths in patients treated by different drugs during clinical trials and even after their marketing. Well-known examples of such drugs include for instance cerivastatin, fialuridine, perhexiline, pirprofen, and troglitazone [1, 9, 10]. For pharmaceutical industries, interruption of clinical trials or drug withdrawal after marketing can lead to huge financial loss and long-term image-tarnishing consequences [9, 11].

Whatever its cause (genetic or acquired), severe dysfunction of mitochondria is detrimental for almost all types of cells because these organelles are a turntable of cell metabolism and the major site of energy synthesis via the oxidative phosphorylation (OXPHOS) process [1, 12]. Regarding drug-induced toxicity, it is noteworthy that the list of the pharmaceuticals able to damage mitochondria is growing year after year [1, 4, 9, 13], most probably because drug-induced mitochondrial dysfunction is increasingly sought after by academic teams and pharmaceutical companies. As a matter of fact, many drugs accumulate inside mitochondria favoring their interactions with different targets including enzymes and their cofactors, and the mitochondrial genome [1, 4, 14]. In addition specific mitochondrial transporters mediate import of some drugs such as antiretroviral and anticancer nucleoside analogs [15, 16], cationic amphiphilic molecules such as amiodarone, tacrine, and perhexiline can freely enter the mitochondria by using the transmembrane potential [4, 17]. Consequently, these protonophoric drugs can transitory entail an OXPHOS uncoupling possibly followed by an OXPHOS inhibition resulting from their mitochondrial accumulation [1, 4]. In addition, some drugs can trigger mitochondrial membranes permeabilization, sometimes facilitated by calcium and ROS, leading to the cytoplasmic release of proapoptotic proteins contained in the intermembrane space [18, 19]. Other drugs, such as antiretroviral drugs, can progressively deplete mitochondrial DNA (mtDNA) by directly inhibiting the DNA polymerase  $\gamma$  and/or inducing mtDNA oxidative damage [1, 20, 21].

As a result, the assessment of mitochondrial toxicity is now a major issue, not only allowing to understand the mechanisms of toxicity of different xenobiotics but also to discard the most hazardous ones during drug discovery studies. Liver is one of the main targets as some drugs might preferentially accumulate in liver mitochondria because of their extensive first-pass hepatic extraction [17, 22]. Liver also contains high levels of cytochromes P450

(CYPs), which often contribute to the generation of reactive metabolites presenting mitochondrial toxicity [23, 24]. Numerous studies showed that mitochondrial dysfunction plays a primary role in drug-induced liver injury (DILI) including hepatic cytolysis, steatosis, and steatohepatitis [1, 4, 9, 20, 25, 26]. Therefore, early stage identification of mitochondrion-toxic drugs which might induce liver injury may have ethical and economic impact. Such investigations require the development of predictive in vitro assays [10, 11].

This chapter presents the methods to identify potential mitochondrion-toxic drugs in different types of biological materials. We detail in particular the in vitro methods assessing both integrity and functionality of purified mouse liver mitochondria [27] as well as cellular and mitochondrial alterations on cultured hepatic cells. Most of the assays using soluble sensors are performed in a screening mode for identification of mitochondrion-toxic drugs. However, the in vitro method we discussed here could be used to detect potential drug-induced mitochondrial liability and to understand the involved mechanisms. This chapter points out the importance of the nature of the biological model used in the mitochondrial toxicity assays and of the choice of relevant parameters to improve prediction of DILI in human and develop safer drugs.

---

## 2 Materials

### 2.1 Buffers and Reagents

*Chemicals:* Oligomycin A, rotenone, antimycin A, malonate, *m*-chlorocarbonylcyanide phenylhydrazone (*m*-Cl-CCP), CaCl<sub>2</sub>, Na-glutamate, 2Na-malate, 2Na-succinate, palmitoyl-L-carnitine and reference drugs are purchased from Sigma-Aldrich (St Quentin-Fallavier, France) and kept (50–100 µL samples) in solution either in water, ethanol or DMSO at –20 °C.

*Homogenization buffer:* 300 mM sucrose, 5 mM TES (pH 7.2), 0.2 mM EGTA, 1 mg/mL BSA.

*Swelling buffer:* 200 mM sucrose, 5 mM succinate, 10 mM MOPS pH 7.4, 1 mM K<sub>2</sub>HPO<sub>4</sub>, 2 µM rotenone and 10 µM EGTA supplemented with 1 µM rhodamine 123 (Rh123; Molecular Probes™) for transmembrane potential assay or MitoSOX (Molecular Probes™) for mitochondrial ROS detection. Swelling of mitochondria occurs when both mitochondrial membranes are permeabilized.

*Respiration buffer:* medium A (250 mM sucrose, 30 mM K<sub>2</sub>HPO<sub>4</sub>, 1 mM EGTA, 5 mM MgCl<sub>2</sub>, 15 mM KCl, and 1 mg/mL bovine serum albumin (BSA)) supplemented with respiratory substrates activating complex I (1 mM malate and 12.5 mM glutamate), complex II (25 mM succinate and 2 µM rotenone),

or fatty acid oxidation (FAO) (25  $\mu\text{M}$  palmitoyl-L-carnitine and 1 mM malate) and 1.65 mM ADP.

## 2.2 Detection Systems

### 2.2.1 Polarographic Oxygen Sensors

*Clark type oxygen electrode* (Hansatech Instruments Ltd., Norfolk, UK): The oxygen electrode allows a precise and continuous measurement of dissolved oxygen in magnetically stirred respiratory medium (medium A). The chamber made in clear cast acrylic is connected to a thermoregulated circulating water bath. The samples are incubated in 300  $\mu\text{L}$  of respiratory medium A housed within a borosilicate glass reaction vessel and added with substrates, ADP (causing a sudden burst in oxygen uptake when ADP is converted to ATP), and specific respiratory chain inhibitors using Hamilton-type syringe. Typically, after inhibition by oligomycin A, oxygen consumption is restored by addition of the OXPHOS uncoupler *m*-Cl-CCP which leads to a permanently high rate of  $\text{O}_2$  consumption due to proton leak [28].

*Red-Flash technology* (Pyro-Science, Aachen, Germany):  $\text{O}_2$  consumption can be alternatively measured using the new Red-Flash technology. This technique relies on the use of an optic fiber equipped with a membrane coated with a fluorescent dye excitable with an orange-red light and showing an oxygen-dependent fluorescence in the near infrared [29, 30]. The experimental conditions are similar to  $\text{O}_2$  consumption measurements with Clark electrode but adapted to lower incubation volumes (30–50  $\mu\text{L}$ ).

### 2.2.2 Soluble Sensors

Various fluorescent probes can be used to measure potential mitochondrial alterations.

*Rhodamine 123* (Molecular Probes™, ThermoFisher Scientific, Courtaboeuf, France): Rh123 is used on isolated mitochondria to follow in real-time mitochondrial transmembrane potential changes by spectrofluorimetry ( $\lambda_{\text{Excitation}}$  485 nm;  $\lambda_{\text{Emission}}$  535 nm). Mitochondrial potential due to proton gradient induces accumulation and quenching of Rh123 fluorescence (decrease fluorescence). Conversely an increase of fluorescence (corresponding to a dye release from mitochondria) potentially brings about by addition of a drug will reflect and be proportional to a loss of the mitochondrial membrane potential. The protonophore *m*-Cl-CCP which fully dissipates the proton gradient across the inner mitochondrial membrane is used as control.

*DiOC<sub>6</sub>* (Molecular Probes™, ThermoFisher Scientific, Courtaboeuf, France): This cationic dye accumulates into mitochondria in response to electric potential across the inner mitochondrial membrane. High concentration of dye induces extensive quenching resulting in fluorescence shift that is proportional to the mitochondrial membrane potential. In the context of our platform, DiOC<sub>6</sub> is used on entire cells to measure the end-point transmembrane potential loss by flow cytometry (decrease of fluorescence;  $\lambda_{\text{Excitation}}$  488 nm,  $\lambda_{\text{Emission}}$  530 nm).

*MitoXpress* (Luxcel, Cork, Ireland): This phosphorescent dye is quenched by O<sub>2</sub>, hence the amount of phosphorescence is inversely proportional to amount of extracellular O<sub>2</sub>. When O<sub>2</sub> is consumed by the respiratory chain, the dye is dequenched and phosphorescence is emitted ( $\lambda_{\text{Excitation}}$  380 nm;  $\lambda_{\text{Emission}}$  650 nm). MitoXpress dye allows high throughput measurement of mitochondrial oxygen consumption in real-time by spectrofluorimetry on isolated mitochondria and cells in suspension [31, 32].

*MitoSOX* (Molecular Probes™, ThermoFisher Scientific, Courtaboeuf, France): MitoSOX is a cell-permeant fluorescent dye targeted to mitochondria to measure production of superoxide anions (henceforth referred to as mitochondrial reactive oxygen species or mtROS). When oxidized by superoxide anions, the dye exhibits red fluorescence which can be measured by spectrofluorimetry ( $\lambda_{\text{Excitation}}$ : 510 nm;  $\lambda_{\text{Emission}}$ : 580 nm) or flow cytometry (FL-2: 580 nm).

## 2.3 Biological Models

### 2.3.1 Isolated Mitochondria

Liver mitochondria from 6- to 10-week-old BALB/cByf female mice (Charles River, Saint-Germain-sur-L'arbresle, France) is used to identify direct mitochondrial effects of xenobiotics. Female mice are used instead of male to reduce interindividual variability (Brenner and Borgne-Sanchez, unpublished data; [27]). Female rat liver mitochondria could also be used without significant differences in sensitivity to compounds (tested on ~20 reference drugs; [27]; unpublished data) Liver mitochondria are isolated and purified by isopycnic density-gradient centrifugation in Percoll [27, 33] allowing to obtain pure and stable mitochondrial preparations. Purified organelles resuspended in homogenization buffer (22 mg/mL of proteins) are kept on ice, and used in screening assays in the next 5 h following their preparation. Premature dilution might alter the integrity of mitochondria. To check the quality of mitochondrial preparations, samples are subjected to measurement of spontaneous swelling and transmembrane potential loss in 96-well plates at 37 °C during 30 min in presence of swelling buffer (see Sect. 3.2.1 for procedure). The preparation is considered as stable and suitable for screening assays if the spontaneous swelling and  $\Delta\Psi_m$  loss are below 10% after 30 min at 37 °C (Fig. 1a). In addition, the respiratory control index (RCI) is measured by Clark electrode (see Sect. 3.1.1 for procedure) and has to be above 3 (using succinate as a substrate) to validate respiratory chain functionality (Fig. 1b) [33]. Finally, the forward scatter and side scatter (FSC/SSC) and fluorescence ( $\lambda_{\text{Excitation}}$  488 nm;  $\lambda_{\text{Emission}}$  530 nm) analysis by flow cytometry (FACSCalibur, BD Bioscience, Germany) of the mitochondrial preparation in the presence or absence of MitoTracker™ green (Molecular Probes™, ThermoFisher Scientific, Courtaboeuf, France) indicates the proportion of intact mitochondria and has to be above 95% (Fig. 1c) to ensure mitochondrial stability during the assays.

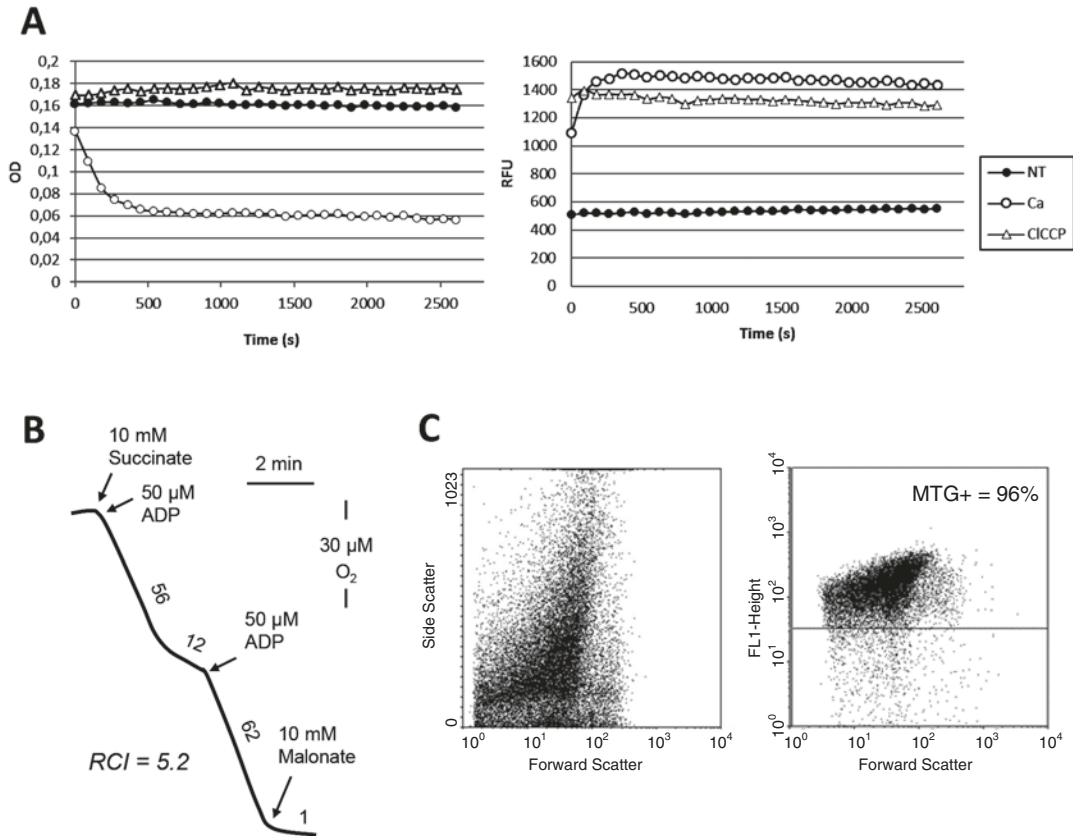


**Fig. 1** Quality controls of purified mouse liver mitochondria. **(a)** Mitochondrial integrity. Spontaneous swelling (0.4%; OD at 550 nm) and  $\Delta\Psi_m$  loss (5%; RFU) are measured by spectrofluorimetry after 30 min incubation at 37 °C in swelling buffer as described in Sect. 3.2.1 and compared to positive controls (50  $\mu\text{M}$   $\text{Ca}^{2+}$  for swelling and 50  $\mu\text{M}$  *m*-Cl-CCP for  $\Delta\Psi_m$  loss; 100% induction). **(b)** Mitochondrial functionality. O<sub>2</sub> consumption by mitochondria (100  $\mu\text{g}$ ) is measured by Clark electrode after addition of the indicated reagents. Numbers along the trace are nmoles of O<sub>2</sub> consumed per minute per milligram of protein. The respiratory control index (RCI) is calculated as indicated in Sect. 3.1.1. **(c)** Purity of mitochondrial fraction. Purified mitochondria are analyzed by flow cytometry after MitoTracker Green labeling (*left panel*: size (FSC)/granulosity (SSC); *right panel*: FSC/FL-1). The percentage of labeled mitochondria (MTG+ events) reflects the purity of the mitochondrial preparation

### 2.3.2 HepaRG Differentiated Cells

The human hepatic HepaRG<sup>®</sup> cell line (Biopredic International, Rennes, France) is a relevant model to investigate liver mitochondrial toxicity induced by parent compounds or their metabolites. These hepatocyte-like cells express xenobiotic metabolizing activities close to those measured in primary human hepatocyte cultures [34]. Therefore, HepaRG cells possess both the metabolic performances of primary hepatocytes and the indefinite growth capacity of hepatic cell lines.

We use undifferentiated HepaRG cells cryopreserved at passage P12 (HPR101). After 2 weeks of proliferation in the HepaRG growth medium (ADD710), cells become confluent

and spontaneously enter into differentiation. The HepaRG differentiation medium (ADD720) subsequently allows the cells to undergo a complete hepatocyte differentiation program within 2 weeks where two cell types (hepatocyte colonies and primitive biliary cells) are present. For compound screening, the growing cells are seeded at  $2 \times 10^4$  cells/cm<sup>2</sup> and treated with compounds during the differentiation phase, for instance for 1, 2, 7, or 12 consecutive days. Renewal of medium and treatment is performed on days 2 and 5 for the 7 day-treatments and on days 3, 5, 7, and 10 for the 12 day-treatments.

To characterize cell metabolism, we measure lactate production (see Sect. 3.1.3) which is dependent on glycolytic activity and glucose concentration in the medium (Fig. 2a). Hence, lactate production is high in HepG2 cells cultured with 4.5 g/L glucose and reduced in HepG2 adapted to galactose. Lactate concentrations are also low in differentiated HepaRG cells grown with glucose (2 g/L). Indeed, even cultured with glucose, HepaRG cells have low glycolytic activity. Regarding mitochondrial activity, RCI measured in mitochondria isolated from HepaRG cells (see Sect. 3.1.1) is around 7 in the presence of succinate and ADP (Fig. 2b). This high RCI presumably reflects high OXPHOS capacity, thus confirming recent investigations [35]. Besides RCI, assessment of the activity of the respiratory chain complexes II and IV is informative because higher activity of complex II compared to complex IV (see Sect. 3.1.2) is characteristic of liver mitochondria [36]. Differentiated HepaRG cells show a high complex II–complex IV ratio closer to primary hepatocytes than HepG2 cells, which have high complex IV activity compared to complex II even in the presence of galactose (Fig. 2c). Hence, differentiated HepaRG cells that rely on the OXPHOS machinery for survival is a valuable model to study drug-induced hepatic mitochondrial dysfunctions [34, 37].

---

## 3 Methods

### 3.1 Quality Controls—Model Characterization

We set up various quality controls to validate the use of our biological models for the detection of mitochondrial dysfunction. Using purified liver mitochondria, RCI is measured to validate the functionality and stability of the mitochondrial preparation. The benefit of using HepaRG cells as a predictive model to detect drug-induced mitochondrial toxicity was validated by demonstrating that culture conditions in glucose recommended by the provider were able to detect such toxicity.

#### 3.1.1 Respiratory Control Index (RCI)

Isolated mitochondria are incubated in a magnetically stirred 1.5 mL cell chamber with a Clark type oxygen electrode thermostated at 37 °C, in 300 µL of respiration buffer with succinate. The

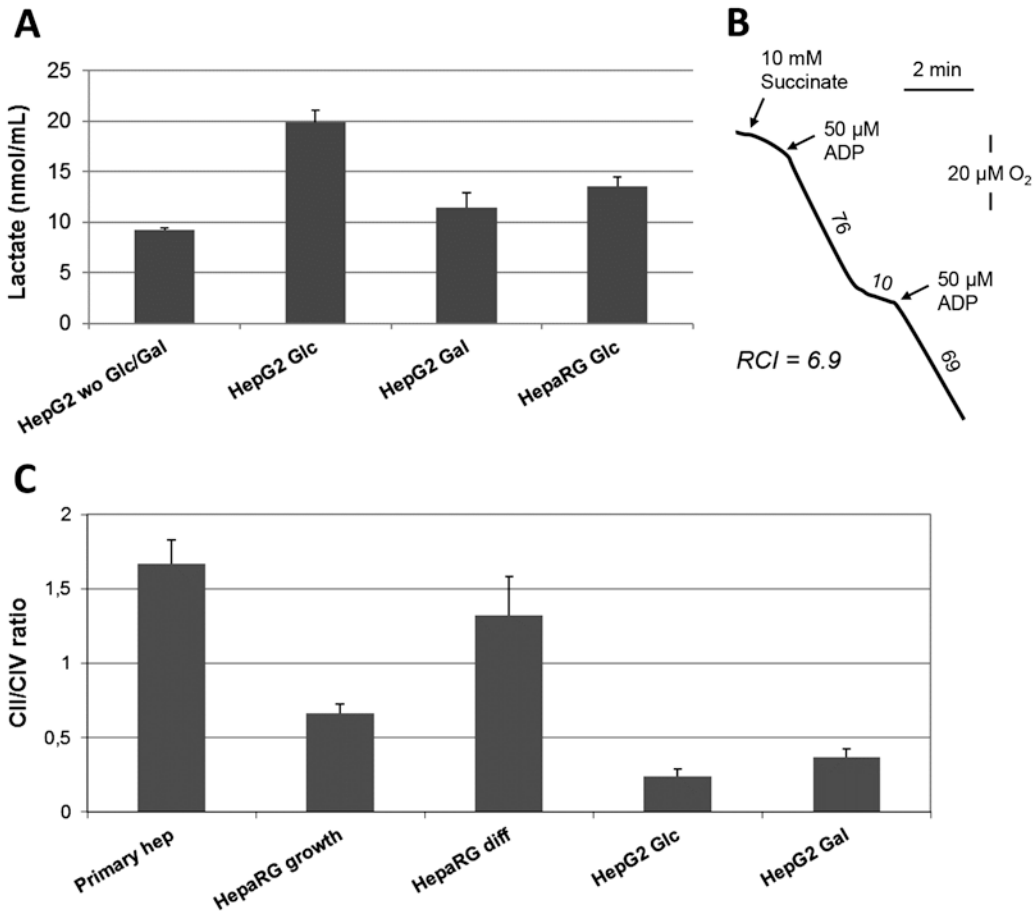


**Fig. 2** Mitochondrial and glycolytic activities in HepaRG and HepG2 cells. (a) Glycolytic activity. Lactate production measured, as described in Sect. 3.1.3, in HepG2 cultured without glucose and galactose (HepG2 wo Glc/Gal), HepG2 cultured in glucose-rich medium (HepG2-Glc), HepG2 adapted in galactose-rich medium (HepG2-Gal) and differentiated HepaRG cells cultured with glucose (HepaRG-Glc) ( $n = 3-4$ , mean  $\pm$  SEM, standard error of mean). (b) Functionality of purified HepaRG mitochondria. O<sub>2</sub> consumption by mitochondria (100  $\mu$ g) is measured by Clark electrode after addition of the indicated reagents. Numbers along the trace are nmoles of O<sub>2</sub> consumed per minute per milligram of protein. The respiratory control index (RCI) is calculated as indicated in Sect. 3.1.1. (c) Respiratory chain activity. Ratios of complex II–complex IV (CII–CIV) activity are measured as indicated in Sect. 3.1.2 in human primary hepatocytes (frozen), cultured growing and differentiated HepaRG cells as well as cultured HepG2-Glc and HepG2-Gal cells ( $n = 4-5$ ; mean  $\pm$  SEM, standard error of mean). A CII–CIV ratio above 1 is characteristic of hepatic cells

addition of a limiting amount of ADP triggers a rapid oxygen uptake characteristic of an active phosphorylating state (state 3; conversion of added ADP to ATP) followed by a slower oxygen uptake rate when all the ADP has been phosphorylated to form ATP (state 4) inducing proton accumulation and respiratory chain inhibition. RCI, which is the [state 3 rate]–[state 4 rate] ratio, reflects the coupling between oxidizing and phosphorylating

processes. Hence, a high RCI reliably indicates the integrity and functionality of the mitochondrial preparation.

### 3.1.2 Respiratory Chain Complex Activity

Measurements of the respiratory chain complex activity are adapted from Bénit et al. [38] to frozen primary human hepatocytes (Biopredic International, Rennes, France), growing and differentiated HepaRG cells and HepG2 cells (CRL-10741; LGC Standards, Molsheim, France) cultured in glucose or adapted to galactose. For complex II activity (EC 1.3.5.1), the cells are trypsinized, permeabilized with low digitonin and incubated at 37 °C in 10 mM  $\text{KH}_2\text{PO}_4$  buffer (pH 7.2) with lauryl maltoside, 5 mM succinate, 100  $\mu\text{M}$  oxidized decylubiquinone, 300  $\mu\text{M}$  potassium cyanide, and 40  $\mu\text{M}$  DCPIP (dichlorophenolindophenol sodium) in 96-well plates. Activity of this complex is measured in real-time by spectrophotometry by following the decreased absorbance of DCPIP at 600 nm (Tecan Infinite 200). For measurement of complex IV activity (EC 1.9.3.1), cells are incubated at 37 °C in  $\text{KH}_2\text{PO}_4$  buffer (pH 7.2) with lauryl maltoside and 25  $\mu\text{M}$  dithionite-reduced cytochrome *c* in 96-well plates. Activity of this complex is measured in real-time by spectrophotometry at 550 nm. As previously mentioned, higher activity of complex II compared to complex IV is characteristic of liver mitochondria [36].

### 3.1.3 Glycolytic Activity

After deproteinization of samples, 96-well plates are kept at  $-80$  °C until use. Lactate levels are then measured by spectrofluorimetry (Tecan Infinite 200,  $\lambda_{\text{Excitation}}$  535 nm;  $\lambda_{\text{Emission}}$  580 nm) using the Lactate Fluorometric assay kit (BioVision, ENZO Life Science, Villeurbanne, France) according to the supplier's recommendations.

## 3.2 Assessment of Acute and Direct Mitochondrial Toxicity

In order to determine whether compounds can be rapidly and directly toxic on mitochondria, we classically assess a combination of parameters in purified mouse liver mitochondria (MiToxView®) [27, 28].

### 3.2.1 Swelling/ Transmembrane Potential

Compounds (2× final concentrations) are distributed in 96-well plate in 100  $\mu\text{L}$ /well swelling buffer. Mitochondria (22  $\mu\text{g}$ ) and Rh123 (2  $\mu\text{M}$ ) are mixed in 100  $\mu\text{L}$  swelling buffer and added to each well. Absorbance (swelling; Optical Density (OD) at 550 nm) and Rh123 fluorescence ( $\Delta\Psi_{\text{m}}$  loss; relative fluorescence unit (RFU) at  $\lambda_{\text{Excitation}}$  485 nm;  $\lambda_{\text{Emission}}$  535 nm) are recorded at 37 °C in real-time during 45 min using a spectrofluorimeter. Results are expressed in percent of induction after normalization by negative control (untreated mitochondria; 0% induction) and positive control (50  $\mu\text{M}$   $\text{Ca}^{2+}$  for swelling and 50  $\mu\text{M}$  *m*-Cl-CCP for  $\Delta\Psi_{\text{m}}$  loss; 100% induction).

### 3.2.2 Oxygen Consumption

MitoXpress dye (200 nM) is diluted in 50  $\mu\text{L}$  of respiration buffer (medium A supplemented with 4× concentrated respiratory substrates and ADP) and distributed to each well of a 96-well plate. Compounds (4× final concentrations) are distributed in 96-well

plate in 50  $\mu\text{L}$  of medium A per well before distribution of the mitochondria (100  $\mu\text{g}$ ) diluted in 100  $\mu\text{L}$  of medium A. Then, 100  $\mu\text{L}$  of mineral oil is added to each well to avoid oxygen balance between ambient air and respiration reaction.  $\text{O}_2$  consumption is measured in real-time during 45 min at 37  $^\circ\text{C}$  by spectrofluorimetry ( $\lambda_{\text{Excitation}}$  380 nm;  $\lambda_{\text{Emission}}$  650 nm). Results are expressed in percent of inhibition after normalization by negative control (untreated mitochondria; 0% inhibition) and positive control (25 mM malonate for complex II driven  $\text{O}_2$  consumption; 2  $\mu\text{M}$  rotenone for complex I and FAO driven  $\text{O}_2$  consumption; 100% inhibition).

### 3.3.3 *mtROS Production*

Compounds (2 $\times$  final concentrations) are distributed in 96-well plates in 100  $\mu\text{L}$  swelling buffer per well. Mitochondria (44  $\mu\text{g}$ ) and MitoSOX Red dye (4  $\mu\text{M}$ ) are mixed in 100  $\mu\text{L}$  swelling buffer and added to each well at 37  $^\circ\text{C}$ . Fluorescence is recorded for 45 min by spectrofluorimetry ( $\lambda_{\text{Excitation}}$  510 nm;  $\lambda_{\text{Emission}}$  590 nm). Results are expressed in percent of ROS production after normalization by negative control (untreated mitochondria; 0%) and positive control (10  $\mu\text{M}$  antimycin A; 100% ROS production).

## 3.3 Mitochondrial Toxicity in HepaRG Cells

In order to determine whether compounds or their metabolites can be toxic on mitochondria, in particular after several days of treatment, we classically assess a combination of parameters in cultured differentiated HepaRG cells.

### 3.3.1 *Transmembrane Potential*

After treatment, the differentiation medium is removed and the cells are labeled with the DiOC<sub>6</sub> dye diluted at 10 nM in differentiation medium for 20 min at 37  $^\circ\text{C}$  in a humidified 5%  $\text{CO}_2$  incubator. Cells are trypsinized for the measurement of mitochondrial membrane potential ( $\Delta\Psi_{\text{m}}$ ) which is detected as an end-point measurement by flow cytometry (FACSCalibur, BD Biosciences;  $\lambda_{\text{Excitation}}$  488 nm;  $\lambda_{\text{Emission}}$  530 nm). Results are expressed in percent of potential loss after normalization by negative control (untreated cells; 0%) and positive control (1  $\mu\text{M}$  staurosporine for 24 h; 100%  $\Delta\Psi_{\text{m}}$  loss). In case of interference with the DiOC<sub>6</sub> dye, JC-1 (5,50,6,60,-tetrachloro 1,1,3,30-tetraethylbenzimidazolylcarbocyanine iodide; Molecular Probes<sup>TM</sup>) can be alternatively used ( $\lambda_{\text{Excitation}}$  488 nm;  $\lambda_{\text{Emission}}$  530 and 580 nm for low and high  $\Delta\Psi_{\text{m}}$ , respectively).

### 3.3.2 *Global Oxygen Consumption (Cell Respiration)*

After treatment, cells are harvested with trypsin, loaded in 96-well plates and kept at room temperature in 50  $\mu\text{L}$  differentiation medium. After addition of the MitoXpress dye (100 nM) diluted in 50  $\mu\text{L}$  of respiration buffer, mineral oil is added and the oxygen consumption is immediately measured in real-time by spectrofluorimeter ( $\lambda_{\text{Excitation}}$  380 nm;  $\lambda_{\text{Emission}}$  650 nm). Results are expressed in percent of inhibition after normalization by negative control (untreated cells; 0%) and positive control (2  $\mu\text{M}$  rotenone added at T0; 100% inhibition).

### 3.3.3 ADP/ATP Ratio

After treatment, cells are loaded in 96-well plates and permeabilized in order to measure the ATP and ADP levels using the ApoSENSOR kit (BioVision, ENZO Life Science, Villeurbanne, France) according to the supplier's recommendations. The changes in ADP/ATP ratios have been used to identify metabolism imbalance and cell death [39]. The enzyme luciferase catalyzes the formation of light from ATP and luciferin. ADP levels are measured by ADP conversion to ATP that is subsequently detected using the same reaction. The light is measured using a luminometer. Results are expressed in percent of inhibition after normalization by negative control (untreated cells; 0%) and positive control (10  $\mu$ M antimycin A; 100% ADP–ATP ratio alteration).

### 3.3.4 Quantification of mtDNA

Because drug-induced mtDNA depletion classically occurs after several days of treatment [14, 21], we measure mtDNA levels after 12 days. To this end, cells are trypsinized and pelleted before isolation of total DNA and amplification by qPCR (Mx3005 Pro thermocycler; Agilent). Primers and Taqman probes targeting mitochondrial DNA (ND1; forward primer: ccctaaaccgccacatct; reverse primer: gagcgatggtgagagctaaggt; Taqman probe: ccaccctctacatcaccgcc) and nuclear DNA (GAPDH; forward primer: ctccacacacatgcactta; reverse primer: cctagtcccagggtttgatt; Taqman probe: aaaagagctaggaaggacaggcaacttggc) are used to respectively measure mitochondrial DNA and nuclear DNA for normalization. The  $2^{-\Delta\Delta C_t}$  method is used to assess the relative mtDNA levels.

## 3.4 Determination of Mitochondrial-Toxicity

In all assays, efficient drug concentrations inducing 20% of the effect ( $EC_{20}$ ) are determined in comparison to the 100% baseline obtained with their respective positive controls.  $EC_{20}$  calculations are done on at least three replicates of treatment (three mitochondrial purifications or three cell passages) by using a nonlinear regression in Graphpad Prism4. A drug is considered as mitochondrion-toxic if the  $EC_{20}$  is  $\leq 100 \times C_{max}$  (maximal plasma concentration) for at least one of the five abovementioned parameters assessed in purified mitochondria [27], or at least one parameter among transmembrane potential, global  $O_2$  consumption, and mtDNA levels in HepaRG cells [40, 41].

## 3.5 Glutathione Levels in HepaRG Cells

Although it is not a mitochondrial parameter per se we can measure intracellular glutathione levels as reliable oxidative stress marker. After treatment, cells are loaded in 96-well plates in order to measure total glutathione (i.e., reduced glutathione [GSH] + oxidized glutathione [GSSG]) and only GSSG, respectively in two different wells. Difference in values obtained in both wells allows to determine GSH levels. Measurements are performed by luminescence (Tecan Infinite 200) using the GSH/GSSG-Glo™ Assay (Promega, France), according to the supplier's

recommendations. Results are expressed in percent of GSH depletion after normalization by negative control (untreated cells; 0%) and positive control (100  $\mu$ M buthionine-sulfoximine; 100%).

---

## 4 Discussion/Note

### 4.1 *Comparison with Other Detection Systems*

The use of fluorescent probes is convenient to screen compounds as the assays can be done in 96- or 384-well plate-based format. It is well adapted to cell lines or isolated liver mitochondria because the biological material is not limiting. Indeed, MitoXpress requires relatively large cell amounts (around 200,000 cells/well in 96-well plates with detection by Tecan Infinite 200) in order to measure global cell respiration. Oxygraphs (Hansatech or Oroboros) require more cells ( $10^6$  cells/measurement) due to their large chamber volume (250  $\mu$ L to 1 mL) but offer flexibility which allows extensive characterization of the respiratory chain activity by sequential addition of reagents in the medium during recording. The highly sensitive Red-Flash technology [29, 30] presents similar advantages although it allows measurement of  $O_2$  consumption in less than 50  $\mu$ L sample volumes. This is convenient in case of precious samples (patient tissues, primary cells, iPS-derived cells). However so far, commercially available Red-Flash devices appear better adapted to study a limited number of samples simultaneously (2–4). It is important to mention here that oxygraphy helps in case of fluorescent or colored (yellow) compounds which usually interfere with fluorescent probes, specifically with MitoXpress [27]. However, compound screening using oxygen consumption is hardly feasible by using oxygraph or Red-Flash technologies.

Finally, the extracellular flux (XF) analyzer (Agilent Technologies, Santa Clara, USA) allows real-time monitoring of the  $O_2$  consumption rate and extracellular acidification rate in intact cells, thus combining the evaluation of OXPHOS activity and glycolysis. This technique, using a disposable sensor cartridge embedded with 96 pairs of fluorescent biosensors, thus permits a first stage identification of potential mitochondrion-toxic compounds. However, further experiments performed in isolated mitochondria should be done in order to determine whether mitochondrial dysfunction detected with this screening tool is a primary event, or only a distant consequence of upstream cellular events.

### 4.2 *Comparison with Other Hepatic Cellular Models*

The choice of the biological model is obviously of primary importance in order to study drug-induced mitochondrial dysfunction. If purified mouse liver mitochondria are useful for the identification of acute effects of parent drugs [27], long term effects or metabolite toxicity require the use of cellular assays. Primary human hepatocytes are classically used to assess mitochondrial dysfunction and cellular toxicity [32] but their use is limited due to the scarcity of liver donors, absence of cell

amplification and variability between batches (for instance, secondary to different polymorphisms, preexisting liver diseases and treatments). HepG2 hepatocarcinoma cells are commonly used in toxicity assays because of their easy culture and clonal origin leading to reproducible response. However, under standard culture conditions in glucose rich-medium, HepG2 cells mainly produce ATP by glycolysis (Crabtree effect) while OXPHOS activity and FAO are maintained at a low rate [35, 42], making these cells mostly resistant to mitochondrion-toxic compounds. Their growth in galactose circumvents the Crabtree effect [43] and allows these cells to become susceptible to mitochondrial inhibition [44]. However, even when adapted to galactose medium (shift to OXPHOS machinery), they might conserve some characteristics of tumor cells, for example regarding the Bcl-2 family protein profile [33]; unpublished data) and respiratory chain activity (Fig. 2c). Indeed, tumor cells are “ready for death” and their sensitivity to compounds can be different from healthy hepatocytes. Moreover, HepG2 cells present limited biotransformation capabilities, although this feature can greatly vary between the sources of HepG2 cell lines [45]. Nonetheless, HepG2 cells express an incomplete repertoire of xenobiotic-metabolizing enzymes (XME) compared to primary human hepatocytes and HepaRG cells [37, 46]). In most cases, the Glucose-Galactose assay is based on measurement of cellular parameters such as cell growth or ATP content over short periods of treatment [44, 47]. A clear difference of response between both conditions helps to identify if mitochondrial toxicity is a dominant pathway [44]. However, this strategy fails to detect mitochondrion-toxic drugs with long-term effects and/or toxicity mediated by XME-generated metabolites [47].

Since almost 7 years, additionally to isolated mitochondria, we use the well-established HepaRG cell line in order to detect mitochondrial liability. Indeed, differentiated HepaRG cells present (even in glucose medium) low glycolytic activity (Fig. 2a) and high OXPHOS capacities with a high respiratory control index (RCI about 7) using succinate as a substrate (Fig. 2b; [35]). Moreover, the complex II–complex IV activity ratio of differentiated HepaRG cells is close to the one observed in primary hepatocytes, this being not true for HepG2 cells (even adapted to galactose) (Fig. 2c). In addition, HepaRG cells offers the advantage of a cell line with drug metabolism capacities close to those of primary hepatocytes [34, 37, 48]. Measurements of transmembrane potential, oxygen consumption, ATP/ADP ratio, GSH depletion, and mtDNA depletion during time course of treatment can help to identify drugs with moderate but significant mitochondrial toxicity but also drug-induced cytotoxicity unrelated to primary mitochondrial dysfunction (for instance, secondary to oxidative stress). These assays in HepaRG cells nicely complement screening assays on purified mitochondria on

**Table 1**  
**Multiparametric study in purified liver mitochondria combined with time-course treatments in differentiated HepaRG cells**

	Liver mitoch.	HepaRG 2d	HepaRG 7d	HepaRG 12d
Class #1				
Class #2				
Class #3				
Class #4				
Class #5				

Assessment of drug-induced toxicity in isolated mouse liver mitochondria (swelling,  $\Delta\Psi_m$  loss,  $O_2$  consumption driven by CI, CII, and FAO, mtROS production) combined with time-course treatments in differentiated HepaRG cells ( $\Delta\Psi_m$  loss, global  $O_2$  consumption, ADP-ATP ratio, GSH, mtDNA) can allow the identification of mitochondrion-toxic compounds with DILI risk. Mitochondrial toxicity was determined as indicated in Sect. 3.4. When taking into account all these parameters, compounds can tentatively be classified in five classes: Class #1: compounds with direct and acute mitochondrial toxicity due to the parent drug (i.e., amiodarone, lovastatin, lumiracoxib, perhexiline, saquinavir, and troglitazone); Class #2: compounds with direct mitochondrial toxicity of a reactive metabolite (i.e., acetaminophen, mercaptopurine); Class #3: compounds with direct but long-term mitochondrial toxicity (i.e., fialuridine, zalcitabine, and zidovudine); Class #4: compounds with rapid cytotoxic effect inducing downstream mitochondrial damages; Class #5: compounds with no apparent mitochondrial toxicity (i.e., amantadine). Color code: red: strong effect (toxicity  $\geq 50\%$  of the respective positive control of mitochondrial liability); pink: moderate effect ( $20\% < \text{toxicity} < 50\%$ ); orange: low effect (toxicity  $\leq 20\%$ ); white: no effect. 2, 7, and 12 days correspond to 2, 7, and 12 day-treatment, respectively

which respiratory chain complex activity can also be measured if inhibition of  $O_2$  consumption is detected. Table 1 provides an illustration of what can be obtained in term of identification of mitochondrial toxicants and understanding of their mechanisms of toxicity by using this strategy. Indeed, the multiparametric screen in mouse liver mitochondria combined with time-course treatment in HepaRG cells may allow the distinction between: (1) direct and acute mitochondrial toxicity of the parent drug, (2) direct mitochondrial toxicity of a reactive metabolite, (3) direct but long-term mitochondrial toxicity, and (4) rapid cytotoxic effect with downstream mitochondrial damages. Such strategy can be used in order to detect drug-induced mitochondrial toxicity at drug discovery stage or during preclinical development, thus being useful to adapt drug development strategy (modifications of drug chemical structure, use of specific mouse models, ...).

## 5 Conclusion and Future Directions

Given the importance of drug-induced mitochondrial toxicity in DILI [49], a great deal of efforts has been made in the last decade to develop predictive tools and assays to study drug-induced mitochondrial dysfunction in vitro [10]. The use of fluorescent probes and commercial devices helped to set up screening assays, and thus

nowadays a combination of read-out and biological models improves the prediction of drug toxicity risk in human [47, 50].

Our platform combines multiparametric assays on both purified hepatic mitochondria and cultured HepaRG differentiated cells. This strategy allows the detection of direct and acute mitochondrial toxicity of parent drug, their metabolites and/or long-term induced mitochondrial toxicity. Whereas the use of purified mitochondria allows medium-throughput screening (200 compounds/months, at four concentrations in triplicate on five parameters), studies in HepaRG cells are, at the moment, performed in low throughput, i.e., ~22 compounds per month (excluding cell growth period) at four concentrations, three time-points, 4–5 parameters in triplicate. Future development might consist in the combination of 2–3 readouts on the same sample as well as the use of more sensitive probes to reduce cell number per point. To respect the 3R principle, we have developed assays in purified HepaRG mitochondria, which also have the advantage to be close to the human metabolism. Investigation of a large panel of reference drugs on this system might be useful to challenge the sensitivity of human versus rodent mitochondria to drug-induced toxicity. Finally, it will be interesting to measure other mitochondrial parameters in order to better understand the mechanisms whereby drugs can alter mitochondrial function. For instance, we plan to study the mitochondrial FAO pathway with different fatty acids as some drugs can differentially inhibit the oxidation of short-chain, medium chain and long-chain fatty acids [51, 52].

---

## Acknowledgments

This review was supported by a grant from the Agence Nationale de la Recherche (ANR-16-CE18-0010-03 MITOXDRUGS). We are very grateful to Biopredic International (Rennes, France) and especially Dr. Christophe Chesné for providing HepaRG cells for the characterization experiments and Sandrine Camus for recommendations on HepaRG cell culture.

## References

1. Begriche K, Massart J, Robin MA, Borgne-Sanchez A, Fromenty B (2011) Drug-induced toxicity on mitochondria and lipid metabolism: mechanistic diversity and deleterious consequences for the liver. *J Hepatol* 54:773–794
2. Gougeon ML, Penicaud L, Fromenty B, Leclercq P, Viard JP, Capeau J (2004) Adipocytes targets and actors in the pathogenesis of HIV-associated lipodystrophy and metabolic alterations. *Antivir Ther* 9:161–177
3. Varga ZV, Ferdinandy P, Liaudet L, Pacher P (2015) Drug-induced mitochondrial dysfunction and cardiotoxicity. *Am J Physiol Heart Circ Physiol* 309:H1453–H1467
4. Fromenty B, Pessayre D (1995) Inhibition of mitochondrial beta-oxidation as a mechanism of hepatotoxicity. *Pharmacol Ther* 67: 101–154
5. Knockaert L, Descatoire V, Vadrot N, Fromenty B, Robin MA (2011) Mitochondrial

- CYP2E1 is sufficient to mediate oxidative stress and cytotoxicity induced by ethanol and acetaminophen. *Toxicol In Vitro* 25:475–484
6. Lieber CS, DeCarli L, Rubin E (1975) Sequential production of fatty liver, hepatitis, and cirrhosis in sub-human primates fed ethanol with adequate diets. *Proc Natl Acad Sci U S A* 72:437–441
  7. Hardonniere K, Saunier E, Lemarie A, Fernier M, Gallais I, Helies-Toussaint C, Mograbi B, Antonio S, Benit P, Rustin P, Janin M, Habarou F, Ottolenghi C, Lavault MT, Benelli C, Sergeant O, Huc L, Bortoli S, Lagadic-Gossmann D (2016) The environmental carcinogen benzo[a]pyrene induces a Warburg-like metabolic reprogramming dependent on NHE1 and associated with cell survival. *Sci Rep* 6:30776
  8. Jiang Y, Xia W, Yang J, Zhu Y, Chang H, Liu J, Huo W, Xu B, Chen X, Li Y, Xu S (2015) BPA-induced DNA hypermethylation of the master mitochondrial gene PGC-1 $\alpha$  contributes to cardiomyopathy in male rats. *Toxicology* 329:21–31
  9. Labbe G, Pessayre D, Fromenty B (2008) Drug-induced liver injury through mitochondrial dysfunction: mechanisms and detection during preclinical safety studies. *Fundam Clin Pharmacol* 22:335–353
  10. Will Y, Dykens J (2014) Mitochondrial toxicity assessment in industry—a decade of technology development and insight. *Expert Opin Drug Metab Toxicol* 10:1061–1067
  11. Nadanaciva S, Will Y (2011) Investigating mitochondrial dysfunction to increase drug safety in the pharmaceutical industry. *Curr Drug Targets* 12:774–782
  12. Wallace DC, Fan W, Procaccio V (2010) Mitochondrial energetics and therapeutics. *Annu Rev Pathol* 5:297–348
  13. Naven RT, Swiss R, Klug-McLeod J, Will Y, Greene N (2013) The development of structure-activity relationships for mitochondrial dysfunction: uncoupling of oxidative phosphorylation. *Toxicol Sci* 131:271–278
  14. Schon E, Fromenty B (2015) Alteration of mitochondrial DNA in liver diseases, vol 150. Taylor & Francis, New-York
  15. Govindarajan R, Leung GP, Zhou M, Tse CM, Wang J, Unadkat JD (2009) Facilitated mitochondrial import of antiviral and anticancer nucleoside drugs by human equilibrative nucleoside transporter-3. *Am J Physiol Gastrointest Liver Physiol* 296:G910–G922
  16. Lee EW, Lai Y, Zhang H, Unadkat JD (2006) Identification of the mitochondrial targeting signal of the human equilibrative nucleoside transporter 1 (hENT1): implications for interspecies differences in mitochondrial toxicity of fialuridine. *J Biol Chem* 281:16700–16706
  17. Berson A, Renault S, Letteron P, Robin MA, Fromenty B, Fau D, Le Bot MA, Riche C, Durand-Schneider AM, Feldmann G, Pessayre D (1996) Uncoupling of rat and human mitochondria: a possible explanation for tacrine-induced liver dysfunction. *Gastroenterology* 110:1878–1890
  18. Al Maruf A, O'Brien PJ, Naserzadeh P, Fathian R, Salimi A, Pourahmad J (2017) Methotrexate induced mitochondrial injury and cytochrome c release in rat liver hepatocytes. *Drug Chem Toxicol*:1–11
  19. Kowaltowski AJ, Castilho RF, Vercesi AE (2001) Mitochondrial permeability transition and oxidative stress. *FEBS Lett* 495:12–15
  20. Pessayre D, Mansouri A, Berson A, Fromenty B (2010) Mitochondrial involvement in drug-induced liver injury. *Handb Exp Pharmacol*:311–365
  21. Gardner K, Hall PA, Chinnery PF, Payne BA (2014) HIV treatment and associated mitochondrial pathology: review of 25 years of in vitro, animal, and human studies. *Toxicol Pathol* 42:811–822
  22. Mansouri A, Haouzi D, Descatoire V, Demeilliers C, Sutton A, Vadrot N, Fromenty B, Feldmann G, Pessayre D, Berson A (2003) Tacrine inhibits topoisomerases and DNA synthesis to cause mitochondrial DNA depletion and apoptosis in mouse liver. *Hepatology* 38:715–725
  23. Antherieu S, Rogue A, Fromenty B, Guillouzo A, Robin MA (2011) Induction of vesicular steatosis by amiodarone and tetracycline is associated with up-regulation of lipogenic genes in HepaRG cells. *Hepatology* 53:1895–1905
  24. Aubert J, Begriche K, Knockaert L, Robin MA, Fromenty B (2011) Increased expression of cytochrome P450 2E1 in nonalcoholic fatty liver disease: mechanisms and pathophysiological role. *Clin Res Hepatol Gastroenterol* 35:630–637
  25. Lee WM (2003) Drug-induced hepatotoxicity. *N Engl J Med* 349:474–485
  26. Russmann S, Kullak-Ublick GA, Grattagliano I (2009) Current concepts of mechanisms in drug-induced hepatotoxicity. *Curr Med Chem* 16:3041–3053
  27. Porceddu M, Buron N, Roussel C, Labbe G, Fromenty B, Borgne-Sanchez A (2012) Prediction of liver injury induced by chemicals in human with a multiparametric assay on isolated mouse liver mitochondria. *Toxicol Sci* 129:332–345

28. Buron N, Porceddu M, Roussel C, Begriche K, Trak-Smayra V, Gicquel T, Fromenty B, Borgne-Sanchez A (2017) Chronic and low exposure to a pharmaceutical cocktail induces mitochondrial dysfunction in liver and hyperglycemia: differential responses between lean and obese mice. *Environ Toxicol* 32: 1375–1389
29. El-Khoury R, Dufour E, Rak M, Ramanantsoa N, Grandchamp N, Csaba Z, Duvillie B, Benit P, Gallego J, Gressens P, Sarkis C, Jacobs HT, Rustin P (2013) Alternative oxidase expression in the mouse enables bypassing cytochrome c oxidase blockade and limits mitochondrial ROS overproduction. *PLoS Genet* 9:e1003182
30. Bénit P, Chrétien D, Porceddu M, Rustin P, Rak M (2017) A performing, versatile and inexpensive device for oxygen uptake measurement. *J Clin Med* 6(6), pii: E58. doi:10.3390/jcm6060058
31. Will Y, Hynes J, Ogurtsov VI, Papkovsky DB (2006) Analysis of mitochondrial function using phosphorescent oxygen-sensitive probes. *Nat Protoc* 1:2563–2572
32. Dykens JA, Jamieson JD, Marroquin LD, Nadanaciva S, Xu JJ, Dunn MC, Smith AR, Will Y (2008) In vitro assessment of mitochondrial dysfunction and cytotoxicity of nefazodone, trazodone, and buspirone. *Toxicol Sci* 103:335–345
33. Buron N, Porceddu M, Brabant M, Desgue D, Racoeur C, Lassalle M, Pechoux C, Rustin P, Jacotot E, Borgne-Sanchez A (2010) Use of human cancer cell lines mitochondria to explore the mechanisms of BH3 peptides and ABT-737-induced mitochondrial membrane permeabilization. *PLoS One* 5:e9924
34. Guillouzo A, Corlu A, Aninat C, Glaise D, Morel F, Guguen-Guillouzo C (2007) The human hepatoma HepaRG cells: a highly differentiated model for studies of liver metabolism and toxicity of xenobiotics. *Chem Biol Interact* 168:66–73
35. Peyta L, Jarnouen K, Pinault M, Guimaraes C, Pais de Barros JP, Chevalier S, Dumas JF, Maillot F, Hatch GM, Loyer P, Servais S (2016) Reduced cardiolipin content decreases respiratory chain capacities and increases ATP synthesis yield in the human HepaRG cells. *Biochim Biophys Acta* 1857:443–453
36. Chretien D, Rustin P, Bourgeron T, Rotig A, Saudubray JM, Munnich A (1994) Reference charts for respiratory chain activities in human tissues. *Clin Chim Acta* 228:53–70
37. Aninat C, Piton A, Glaise D, Le Charpentier T, Langouet S, Morel F, Guguen-Guillouzo C, Guillouzo A (2006) Expression of cytochromes P450, conjugating enzymes and nuclear receptors in human hepatoma HepaRG cells. *Drug Metab Dispos* 34:75–83
38. Benit P, Goncalves S, Philippe Dassa E, Briere JJ, Martin G, Rustin P (2006) Three spectrophotometric assays for the measurement of the five respiratory chain complexes in minuscule biological samples. *Clin Chim Acta* 374:81–86
39. Bradbury DA, Simmons TD, Slater KJ, Crouch SP (2000) Measurement of the ADP:ATP ratio in human leukaemic cell lines can be used as an indicator of cell viability, necrosis and apoptosis. *J Immunol Methods* 240:79–92
40. Pertuiset C, Porceddu M, Buron N, Camus S, Chesné C, Borgne-Sanchez A (2015) Identification of drug-induced mitochondrial alterations using HepaRG cell line. *Toxicol Lett* 238:S316–S317
41. Porceddu M, Pertuiset C, Camus S, Chesné C, Buron N, Borgne-Sanchez A (2016) In vitro prediction of antiretroviral drug-induced hepatotoxicity by using mitochondrial MiToxView screening platform. *Toxicol Sci* 150:S598
42. Igoudjil A, Massart J, Begriche K, Descatoire V, Robin MA, Fromenty B (2008) High concentrations of stavudine impair fatty acid oxidation without depleting mitochondrial DNA in cultured rat hepatocytes. *Toxicol In Vitro* 22:887–898
43. Rossignol R, Gilkerson R, Aggeler R, Yamagata K, Remington SJ, Capaldi RA (2004) Energy substrate modulates mitochondrial structure and oxidative capacity in cancer cells. *Cancer Res* 64:985–993
44. Marroquin LD, Hynes J, Dykens JA, Jamieson JD, Will Y (2007) Circumventing the Crabtree effect: replacing media glucose with galactose increases susceptibility of HepG2 cells to mitochondrial toxicants. *Toxicol Sci* 97:539–547
45. Hewitt NJ, Hewitt P (2004) Phase I and II enzyme characterization of two sources of HepG2 cell lines. *Xenobiotica* 34:243–256
46. Guo L, Dial S, Shi L, Branham W, Liu J, Fang JL, Green B, Deng H, Kaput J, Ning B (2011) Similarities and differences in the expression of drug-metabolizing enzymes between human hepatic cell lines and primary human hepatocytes. *Drug Metab Dispos* 39:528–538
47. Hynes J, Nadanaciva S, Swiss R, Carey C, Kirwan S, Will Y (2013) A high-throughput dual parameter assay for assessing drug-induced mitochondrial dysfunction provides additional predictivity over two established mitochondrial toxicity assays. *Toxicol In Vitro* 27:560–569
48. Michaut A, Le Guillou D, Moreau C, Bucher S, McGill MR, Martinais S, Gicquel T, Morel I, Robin MA, Jaeschke H, Fromenty B (2016) A cellular model to study drug-induced liver

- injury in nonalcoholic fatty liver disease: application to acetaminophen. *Toxicol Appl Pharmacol* 292:40–55
49. Pessayre D, Fromenty B, Berson A, Robin MA, Letteron P, Moreau R, Mansouri A (2012) Central role of mitochondria in drug-induced liver injury. *Drug Metab Rev* 44:34–87
  50. Nadanaciva S, Rana P, Beeson GC, Chen D, Ferrick DA, Beeson CC, Will Y (2012) Assessment of drug-induced mitochondrial dysfunction via altered cellular respiration and acidification measured in a 96-well platform. *J Bioenerg Biomembr* 44:421–437
  51. Fromenty B, Freneaux E, Labbe G, Deschamps D, Larrey D, Letteron P, Pessayre D (1989) Tianeptine, a new tricyclic antidepressant metabolized by beta-oxidation of its heptanoic side chain, inhibits the mitochondrial oxidation of medium and short chain fatty acids in mice. *Biochem Pharmacol* 38:3743–3751
  52. Freneaux E, Fromenty B, Berson A, Labbe G, Degott C, Letteron P, Larrey D, Pessayre D (1990) Stereoselective and nonstereoselective effects of ibuprofen enantiomers on mitochondrial beta-oxidation of fatty acids. *J Pharmacol Exp Ther* 255:529–535